

Evaluating the Influence of Land Cover Dynamics on Land Surface Temperature in Kano Metropolitan Area, Nigeria

¹Shaibu A.S., ²Youngu T.T. *³Ibrahim A., ⁴Omale D., ³Oduyemi A.T., ³Alagbe A.O., ⁵Asifat J.T. & ⁶Olayiwola K.O.

¹S&S Geomatics Consult

²Department of Geomatics, Ahmadu Bello University, Zaria

³Department of Cartography & GIS, Federal School of Surveying, Oyo

⁴Department of Surveying & Geoinformatics, Confluence University of Science and Technology, Osara, Nigeria

⁵Department of Geography, University of Ilesa, Ilesa

⁶Department of Remote Sensing & Geoscience Information System, Federal University of Technology, Akure.

*Corresponding author: brawnabdulbrahim@fss-oyo.edu.ng

Received: 28/11/2024

Revised: 6/01/2025

Accepted: 4/03/2025

Rapid urbanization significantly alters land use/land cover (LULC) and influences climate dynamics, yet the spatial and temporal variability of land surface temperature (LST) remains insufficiently characterized. A comprehensive understanding of these patterns is essential for assessing urban heat effects and informing sustainable urban planning. This study examines the intricate interplay between LST and LULC dynamics in Kano's metropolitan area over 30 years, highlighting the impacts of rapid urbanization. Using Landsat multispectral satellite imagery, LULC classification via maximum likelihood, and LST extraction through Mono and Split Window algorithms, the study also integrates NDVI computation to analyse spatiotemporal trends for 30 years. The study reveals a significant expansion of built-up areas from 33.8 sq km to 145.13 sq km (79% annual increase), accompanied by a 95% annual rise in LST and a 96% annual decline in NDVI. Strong positive correlations between LST and built-up areas ($r = 0.9768$) and bare land ($r = 0.9566$) highlight their role in temperature elevation, with each square kilometre of built-up expansion contributing 0.1215°C to LST. In contrast, NDVI ($r = -0.9752$) and vegetation show strong negative correlations with LST, reinforcing their cooling effect. These findings emphasize the need for sustainable urban planning, afforestation, and GIS-based monitoring to mitigate urban heat and enhance climate resilience.

Keywords: Land Surface Temperature, Spatiotemporal analysis, Land Use/Land Cover changes, Normalized Difference Vegetation Index, Urban Expansion, Urban Heat, GIS

Introduction

Understanding the pertinent factors shaping Land Surface Temperature (LST) is paramount for elucidating local climate dynamics and environmental changes. Leveraging advancements in remote sensing and Geographic Information Systems (GIS), researchers have gained unprecedented insights into the complex interplay between various influences on LST. This exploration delves into the multifaceted nature of these factors, ranging from land cover types and land use patterns to climatic variables and human activities (Yang *et al.*, 2021; Mohiuddin & Mund, 2024). By synthesizing empirical studies, this investigation aims to uncover key determinants of LST variability across diverse regions and land cover types, ultimately informing evidence-based strategies for mitigating the impacts of urbanization, climate change, and land degradation on local and regional temperature regimes (Daba & You, 2022).

Analysing the spatiotemporal distribution of LST across the Kano Metropolitan Area in Nigeria is critical due to the impacts of rapid urbanization. In many developing countries like Nigeria, urban expansion leads to significant LULC changes, which subsequently alter the local climate and environment

(Tanko, 2018; Koko *et al.*, 2021). One notable outcome of such urbanization is the Urban Heat Island (UHI) effect, where city centres become significantly warmer than surrounding rural areas, causing discomfort and health risks for residents (Nuruzzaman, 2015). UHI can exacerbate heat stress, particularly during heat waves, and studies from the United States estimate that extreme heat accounts for approximately 1,000 deaths annually (Huang & Lu, 2018).

Kano, as one of Nigeria's most densely populated and rapidly urbanizing cities, faces marked LULC shifts characterized by increased impervious surfaces, deforestation, and built-up areas. An influx of immigrants, increasing annually by 30-40% for economic and recreational purposes (Koko *et al.*, 2021), necessitates expanded infrastructure at the cost of vegetative cover. These developments contribute to rising LST patterns, with potential repercussions for the urban microclimate, human well-being, and environmental sustainability. Similar to findings from research in mid- to high-latitude cities, which indicate heightened mortality risk from extreme heat in highly urbanized areas (Yang *et al.*, 2023). Kano's UHI effect is influenced by reduced vegetation, which is

replaced by heat-absorbing artificial surfaces (Aliyu *et al.*, 2017; Tanko & Mohammed, 2018). UHI is a widely observed phenomenon in large cities globally, driven by factors including anthropogenic heat, surface cover, climate, and air pollution (Jabbar *et al.*, 2023). According to UN projections, populous nations like Nigeria are expected to account for 35% of global urban population growth from 2018 to 2050, underscoring the need to address UHI effects (UN, 2018).

While substantial research has examined spatiotemporal LST variations across urban centres, revealing insights into UHI patterns and implications, limited studies have specifically addressed Kano annually. For instance, Umar and Satish (2015) and Tanko *et al.* (2018) investigated UHI effects in Kano but did not analyze annual LST variations, which are crucial for understanding the full extent of urban heat dynamics. Other studies in Nigerian cities, such as those by Zitta and Akinseye (2020) in Jos, have demonstrated the benefits of detailed LST monitoring for sustainable urban planning. Furthermore, recent work by Koko *et al.* (2022) mapped Kano's LULC changes but lacked a detailed annual LST analysis and did not explore correlations with related environmental factors.

This study aims to address these gaps by examining annual spatiotemporal LST variations in Kano over 30 years. Using remote sensing and geospatial techniques, this research will assess the relationship between LST, LULC, and vegetation indices, thereby enabling future LST predictions. The insights gained can aid urban planners and policymakers in anticipating heat stress risks, guiding sustainable urban development, and implementing adaptation

measures to mitigate adverse impacts on human health, ecosystems, and infrastructure.

Study Area

The Kano Metropolitan Area, located in the northern part of Nigeria as shown in Figure 1, is located between latitude ($11^{\circ}59'59.57''$ and $12^{\circ}02'39.57''$) N of the Equator and longitude ($8^{\circ}31'19.69''$ and $8^{\circ}33'19.69''$) E of the Greenwich Meridian (Ibrahim and Mohammed, 2016). It spans approximately 683 square kilometres within Kano State's total area of 20,760 square kilometres. It includes 44 local government areas and has a current population of about 4.49 million, marking significant growth since 1950. Kano is a historical and economic hub, dating back to the 9th century, with urban expansion and population surges, especially since Nigeria's independence. The city's climate is classified as tropical wet and dry with three distinct seasons: cool and dry (November-February), hot and dry (March-mid-May), and wet (mid-May-September), experiencing an average annual rainfall of 800mm, mainly between May and September (Abdullahi *et al.*, 2016).

Vegetation in Kano is semi-arid Sudan Savannah, rich in fauna and flora, suitable for agriculture and livestock rearing. The metropolis includes residential, commercial, and industrial zones, and hosts 34 residential layouts and five government housing estates. Economically, Kano has long been a centre for groundnut production and trade, with essential infrastructures such as railways, Bayero University, and Mallam Aminu Kano International Airport. Historic sites like the Kurmi Market, the Emir's Palace, and the Gidan Makama Museum emphasise Kano's cultural heritage (Ibrahim *et al.*, 2014).

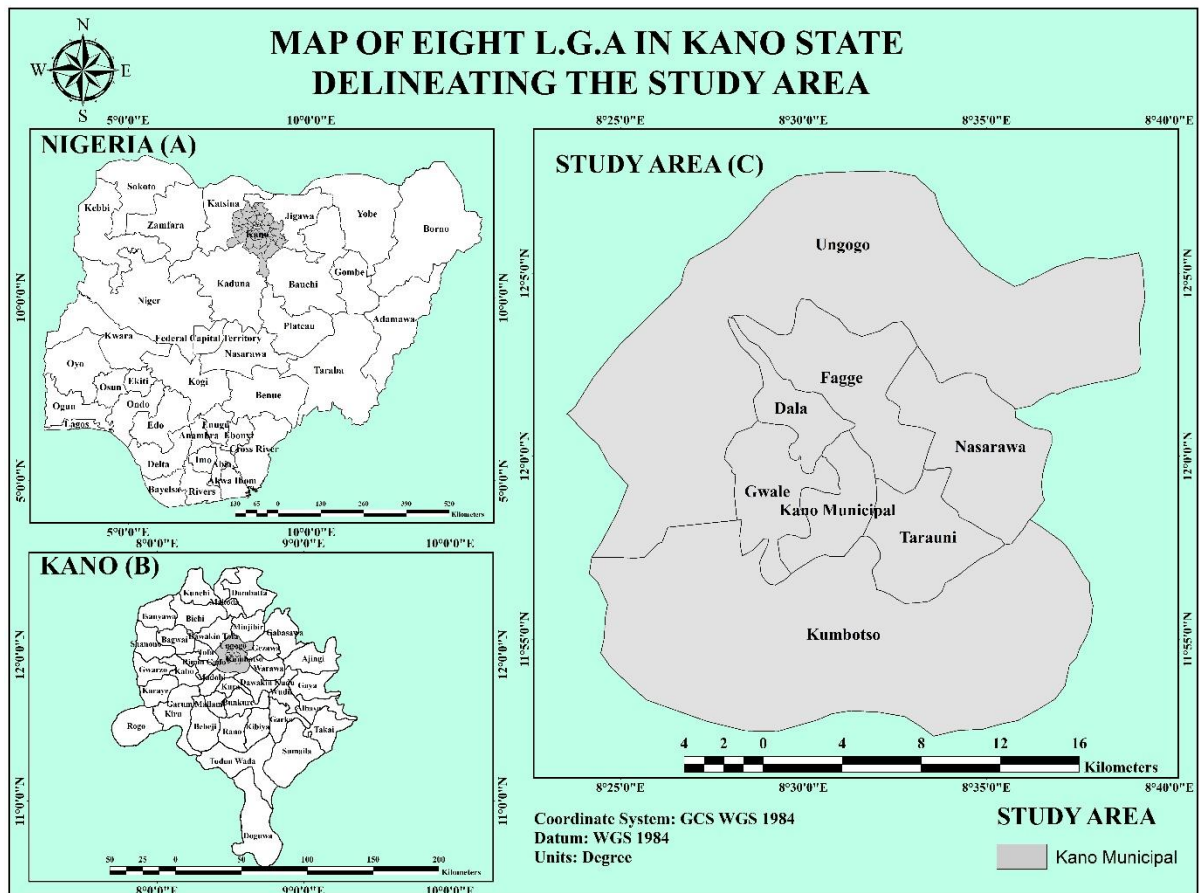


Figure 1: Study Area (A=Map of Nigeria showing Kano State, B = Map of Kano showing the Study Area, C= Area of Interest).

Materials and Methods

The methodology employed to investigate the influence of land use/land cover dynamics on the patterns of LST in the study area entails a geospatial approach to collect and analyse important data. The methodology involves four key stages: data acquisition, data preparation, data processing and data analysis. These stages encompass activities such as

delineating the specific area of interest, processing and enhancing images, digitizing data, and data conversion. Furthermore, satellite imageries were utilized to generate LULC data alongside LST datasets. These datasets were then subjected to geospatial analysis to establish their relationship with other factors and to facilitate predictions. The overall process is summarized in Figure 2.

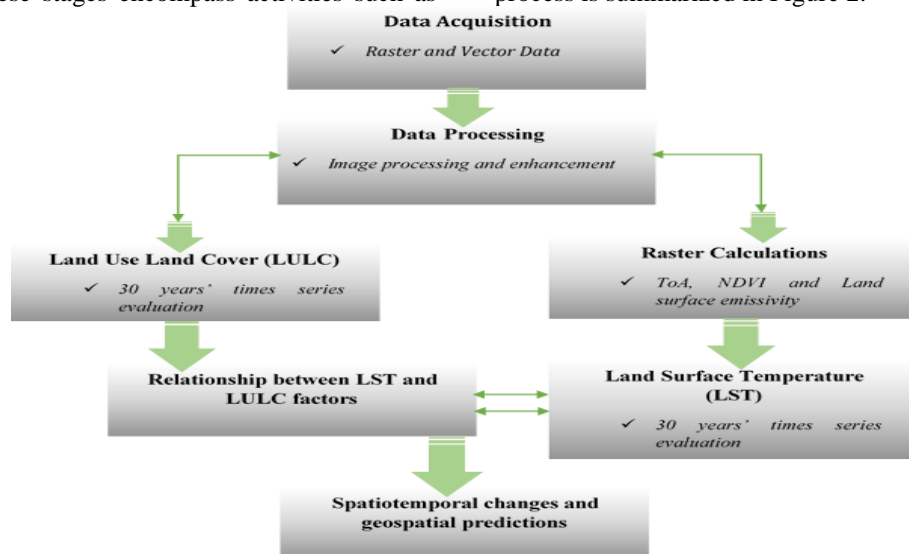


Figure 2: Workflow diagram

Table 1: Datasets and Sources

Data/Date	Source	Description	Purpose
Landsat 4/5/7/8/9 Satellite Imagery Path 188 Row 52 Ephemeris Epoch Year = 2021 Ephemeris Epoch Day = 361 December 2021.	http://earthexplorer.usgs.gov	7/9/11 bands of multispectral image data were acquired by both the Operational Land Imager (OLI) and Thermal Infrared Sensor (TIRS) onboard the Landsat 9 satellite.	Land Use/Land Cover Classification alongside NDVI & LST Estimation. (1991-2021)
Administrati ve Map/ December 2022	http://www.gadm.org/	A map showing political boundaries of Nigeria, its states and local government	Boundary demarcation.
Nigeria Shapefile/ September 2020	http://www.divagis.org/datadown	Complete shape file of Nigeria's boundary and its local government areas	Production of the base map
Google Earth/ January 2022	https://www.google.com/earth/	Extracts of images covering the study area	Verification of classification.

Land use/land cover

This study used Landsat 4, 5, 7, 8, and 9 satellite data with spatial resolutions of 15 to 30 meters to analyse LULC changes in Kano from 1991 to 2021, with most bands at 30 meters resolution and a higher-resolution 15-meter panchromatic band for Landsat 7, 8, and 9. Using this data, the study conducted a spatio-temporal analysis to track urban expansion, vegetation loss, and temperature changes over 30 years. It focused on assigning each pixel to one of four categories: built-up, vegetation, bare land and water body (Ibrahim *et al.*, 2024). The goal is to create thematic maps that simplify the representation of different land cover types. LULC data supports LST analysis by overlaying temperature data on land cover maps, highlighting temperature patterns linked to specific land cover types (Patel *et al.*, 2023; Lai *et al.*, 2020). This integration helps interpret thermal variations due to factors like urbanization, agricultural impact, and vegetation cooling effects, particularly relevant for urban heat analysis.

The satellite dataset was re-projected to the Geographic Coordinate System (GCS_WGS 84) and was pre-processed performing scan error elimination, haze reduction, noise reduction, histogram equalization, and both radiometric and atmospheric corrections, followed by the extraction of the area of interest (Ibrahim *et al.*, 2024). The maximum likelihood supervised classification technique using the interactive supervised classifier in ArcGIS. A minimum Kappa coefficient of 0.8262 out of a possible 1.0000 for accuracy assessment was obtained which is consistent with Foody (2020).

For detailed spatial analysis, classified raster images are converted to vector format, transforming pixel-based data into polygonal representations that retain spatial accuracy. This vector format enables more precise calculations, area measurements, and integration with other spatial data, enhancing the usability of land cover information. ArcGIS Raster to Vector tools facilitate this conversion (Arya *et al.*, 2023).

Land surface temperature/normalised difference vegetation index

The extraction of surface temperature from satellite data in this study was conducted using ArcGIS, where various mathematical transformations were applied. Specifically, bands 10, 5, and 4 from the Landsat imagery were processed within the ArcGIS environment, utilizing the raster calculator for calculations. The procedure followed a step-by-step approach, where the output of one stage served as the input for the next. Initially, the digital numbers (DNs) from the satellite data were converted into top-of-the-atmosphere (ToA) radiance values using a standard equation (Ngie *et al.*, 2016; Sajib & Tao, 2020).

$$ToA = M_L * Q_{cal} + A_L \dots \dots \dots \text{Equation (1)}$$

Where:

M_L = Band-specific multiplicative rescaling factor from the metadata (Radiance_Mult_Band_X, where x is the band number). This value was directly extracted from the metadata.

Q_{cal} = The thermal band

A_L = Band-specific additive rescaling factor from the metadata (Radiance_Add_Band_x, where x is the band number).

The next step was to convert ToA to Brightness Temperature (BT) using equation 2 (Ngie *et al.*, 2016; Sajib & Tao, 2020).

$$BT = \left\{ \frac{k_2}{\ln\left(\frac{k_1}{ToA}\right)} + 1 \right\} - 273.15 \dots \dots \dots \text{Equation (2)}$$

Where:

k_1 = Band-specific thermal conversion constant from the metadata ($K1_Constant_Band_x$, where x is the thermal band number).

k_2 = Band-specific conversion constant from the metadata ($K2_Contant_band_x$, where x is the thermal band number). This is a constant (K2) that was also extracted from the metadata.

Furthermore, the result was converted to Celsius by normalization using 273.15

Thirdly, NDVI was calculated because the proportion of vegetation is related to emissivity. This was achieved using equation (3).

$$NDVI = \frac{NIR (Band 5) - R (Band 4)}{NIR (Band 5) + R (Band 4)} \dots \dots \dots \text{Equation (3)}$$

The fourth step was to calculate the proportion of vegetation (P_y) using equation (4):

$$P_y = Square \left(\frac{NDVI - NDVI_{min}}{NDVI_{max} - NDVI_{min}} \right) \dots \dots \dots \text{Equation (4)}$$

After which Emissivity (e) was calculated using equation (5):

$$e = 0.004 * P_y + 0.986 \dots \dots \dots \text{Equation (5)}$$

This equation was used directly in the raster calculator where 0.986 is the corresponding value for the corrections in the equation, and Finally, LST was calculated using this equation (6)

$$LST = \frac{BT}{1 + \left\{ 0.00115 \frac{BT}{(1.4388)} \right\} \ln(e)} \dots \dots \dots \text{Equation (6)}$$

Where:

0.00115 and 1.4388 are constants. On each Landsat image, at least three bands were used, that is the thermal band, band 4, and band 5. This was conducted on the satellite data of the area for 30 years.

Results and Discussion

This study revealed key spatial and temporal trends in landscape evolution, which are visually represented in Figures 3, 4, and 5.

The Land Use Land Cover (LULC) analysis from 1991 to 2021 shows significant growth, with area coverage increasing from an estimated 36.96 to 145.13 square kilometres. This upward trend, marked by fluctuations and notable shifts in 1994, 2003, and 2013, reflects ongoing urban expansion and land transformation. According to Faisal *et al.* (2021), urban expansion is associated with the persistent reduction of vegetated areas and the emergence of impermeable surfaces. As a consequence, this phenomenon can lead to elevated LST levels in urban centres and cities. The increase in impervious surfaces results in enhanced absorption of solar radiation, leading to a higher conversion of solar energy into heat within the urban environment. This process contributes to the observed rise in LST, which is characteristic of urban areas experiencing extensive expansion.

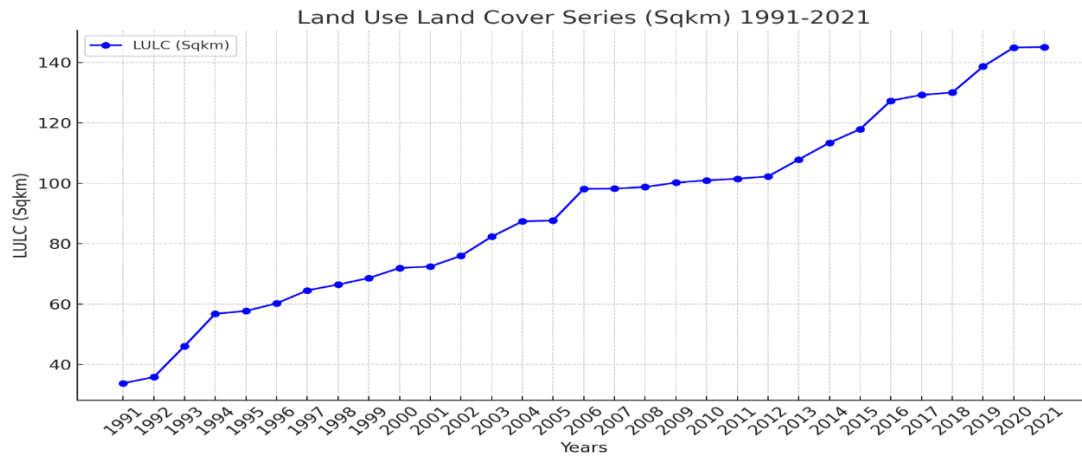


Figure 3: Land Use Land Cover Pattern from 1991 – 2021

Table 2 illustrates the continuous expansion of LULC in Kano metropolis from 33.8 sq km in 1991 to 145.13 sq km in 2021, reflecting rapid urbanization over three decades. The data shows a steady increase, with notable surges between 1993–1994 and 2015–2016, likely due to intensified urban development. By 2010, built-up areas had exceeded 100 sq km, marking a

significant transformation. This growth has critical implications for land surface temperature (LST) and vegetation loss, emphasizing the need for sustainable urban planning and environmental management to mitigate urban heat effects and ecological degradation.

Table 2: Time Series of Land Use Changes

SN	Years	LULC (Sqkm)
1	1991	33.7992
2	1992	35.8115
3	1993	46.0906
4	1994	56.7999
5	1995	57.7098
6	1996	60.2466
7	1997	64.5446
8	1998	66.4663
9	1999	68.6193
10	2000	71.9554
11	2001	72.4392
12	2002	75.9634
13	2003	82.3239
14	2004	87.3891
15	2005	87.6933
16	2006	98.1837
17	2007	98.2278
18	2008	98.7669
19	2009	100.2303
20	2010	100.989
21	2011	101.5137
22	2012	102.2922
23	2013	107.8821
24	2014	113.4405
25	2015	117.9423

26	2016	127.3761
27	2017	129.2931
28	2018	130.069
29	2019	138.6684
30	2020	144.9765
31	2021	145.1343

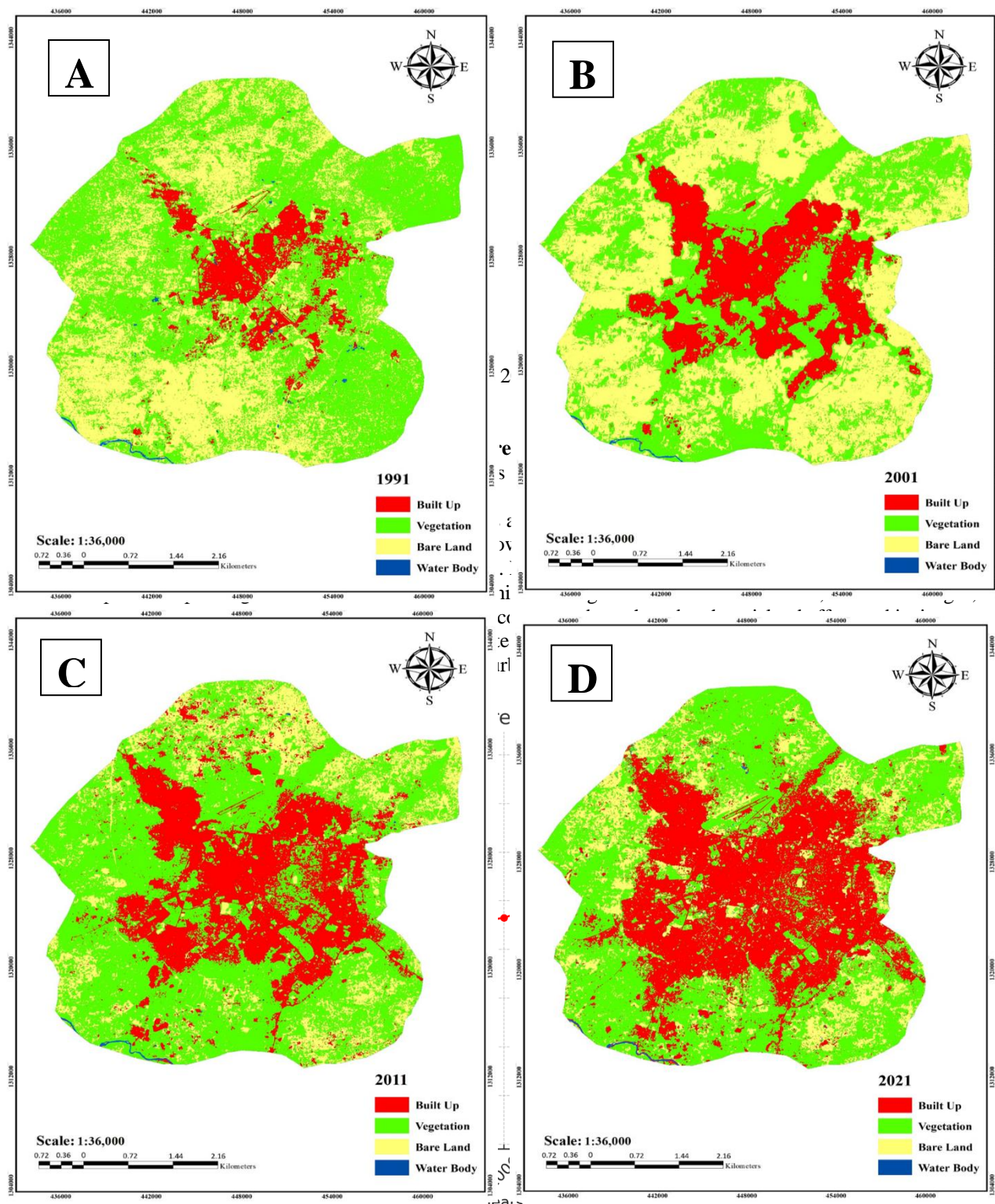


Figure 4: Land Surface Temperature Pattern from 1991 – 2021

Spatio-temporal patterns in land surface temperature

As shown in Figure 5 and Figure 6, The trend analysis of LST in the study area from 1991 to 2021 reveals a consistent increase in temperature.

This can be said to be driven by environmental changes and urbanization. LST values rose steadily from 12.6°C in 1991 to 28.17°C in 2021. Early years (1991–2003) showed modest increases, reaching 20.5°C, while later years (2010 onward) exhibited a

sharper rise, surpassing 23°C. Notably, 2019 and 2020 recorded significant anomalies, with temperatures peaking at 28°C. Potential drivers of this warming trend include urbanization, land-use changes, and vegetation loss. Recent elevated temperatures raise concerns about the urban heat island effect and its impact on local climate and ecological stability. This persistent warming trend underscores the need for proactive measures to mitigate its impact, particularly in rapidly urbanizing areas.

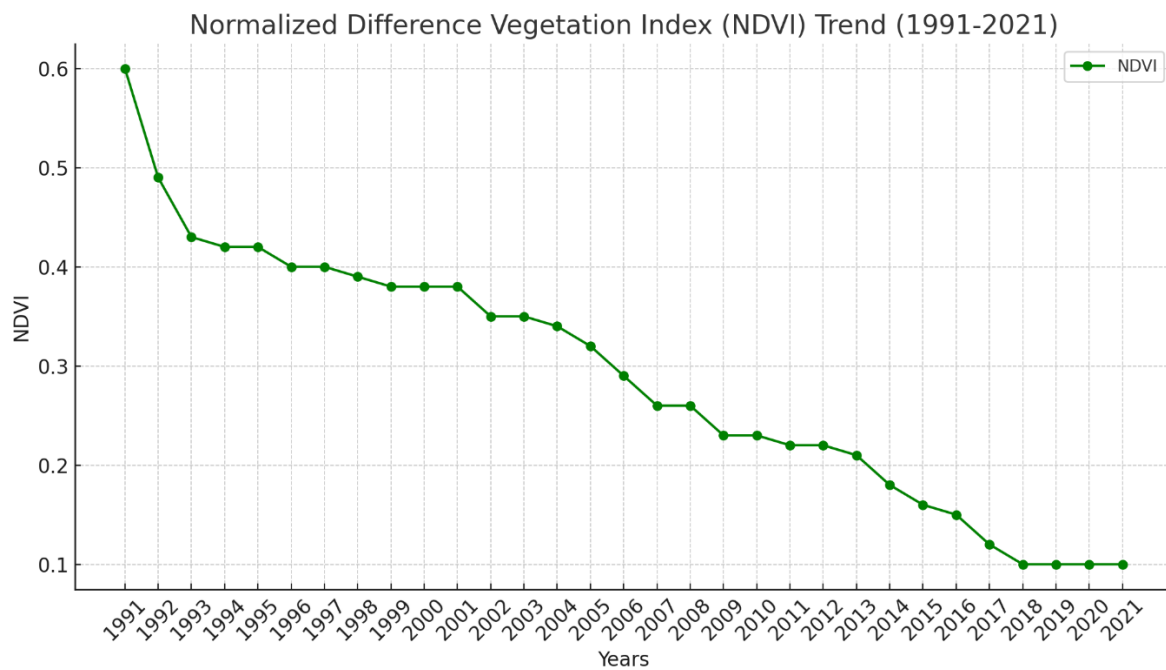


Figure 5: Land Surface Temperature Pattern from 1991 – 2021

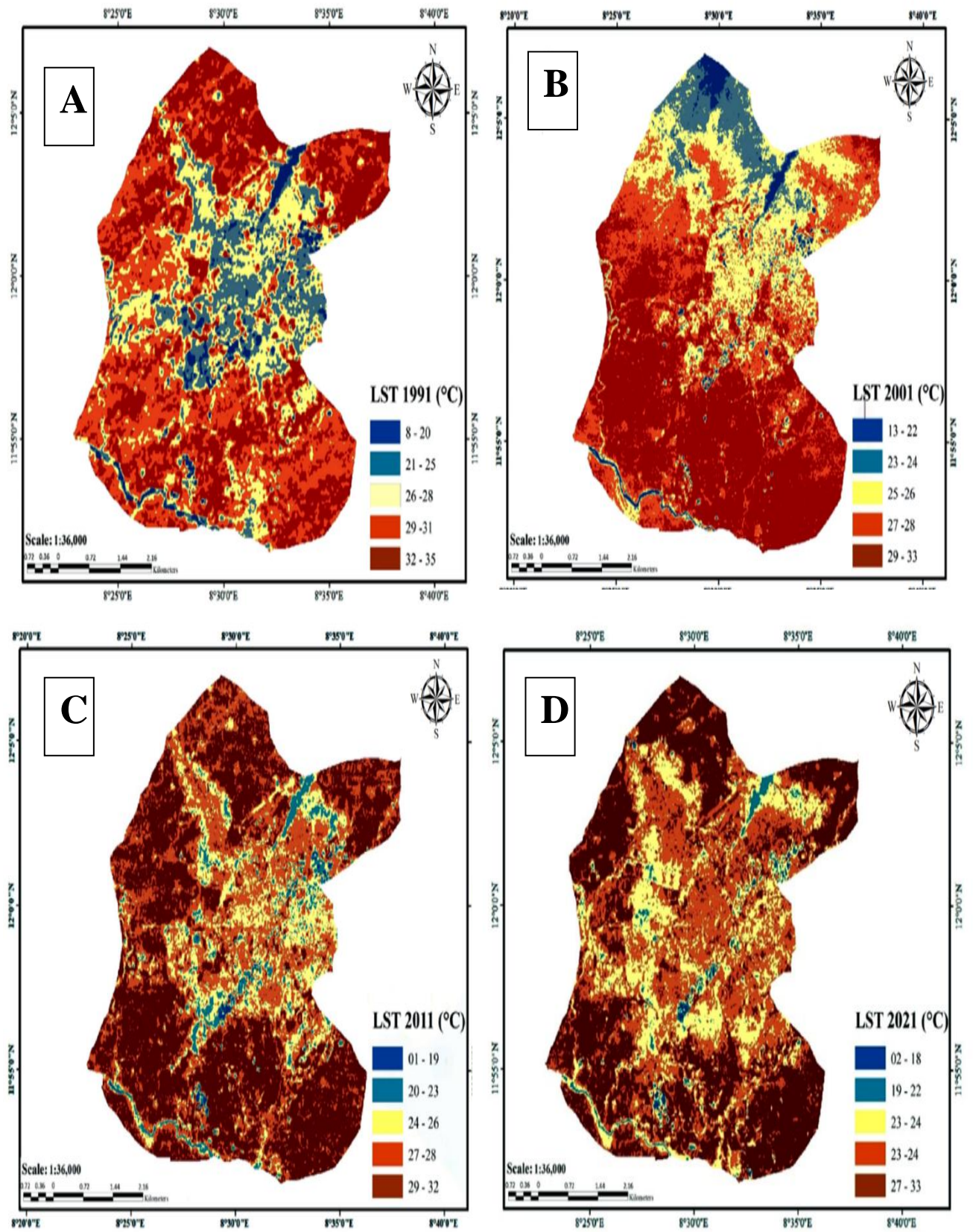


Figure 6: Land Surface Temperature Map Series from 1991 to 2021 (A=LST 1991; B=LST 2001; C=LST 2011; D=LST 2021).

Normalised difference vegetation index from 1991 to 2021

The trend in the Normalized Difference Vegetation Index (NDVI) for the period of 1991 to 2021 reveals notable patterns and changes. The NDVI values range from 0.1 to 0.6 over the years, indicating the vegetative health and density within the study area. From 1991 to around 2002, there seems to be a general consistency in the NDVI values, with slight fluctuations. However, from approximately 2002 to 2014, there was a discernible downward trend in NDVI values as shown in Figure 7. This decline suggests a potential decrease in vegetation density or

health during this period. Notably, the NDVI values are consistently lower during these years, possibly indicating environmental stressors or land use changes that could have affected vegetation. In contrast, from around 2014 to 2021, the NDVI values appear to stabilize at lower levels, indicating a potential stabilization in vegetation health or density. It is important to note that the NDVI values in the later years (2017 to 2021) remain consistently low, possibly indicating a sustained condition of reduced vegetation cover or a shift in land cover types that affect the overall NDVI. Figure 8 shows the NDVI Map from 1991 -2021.

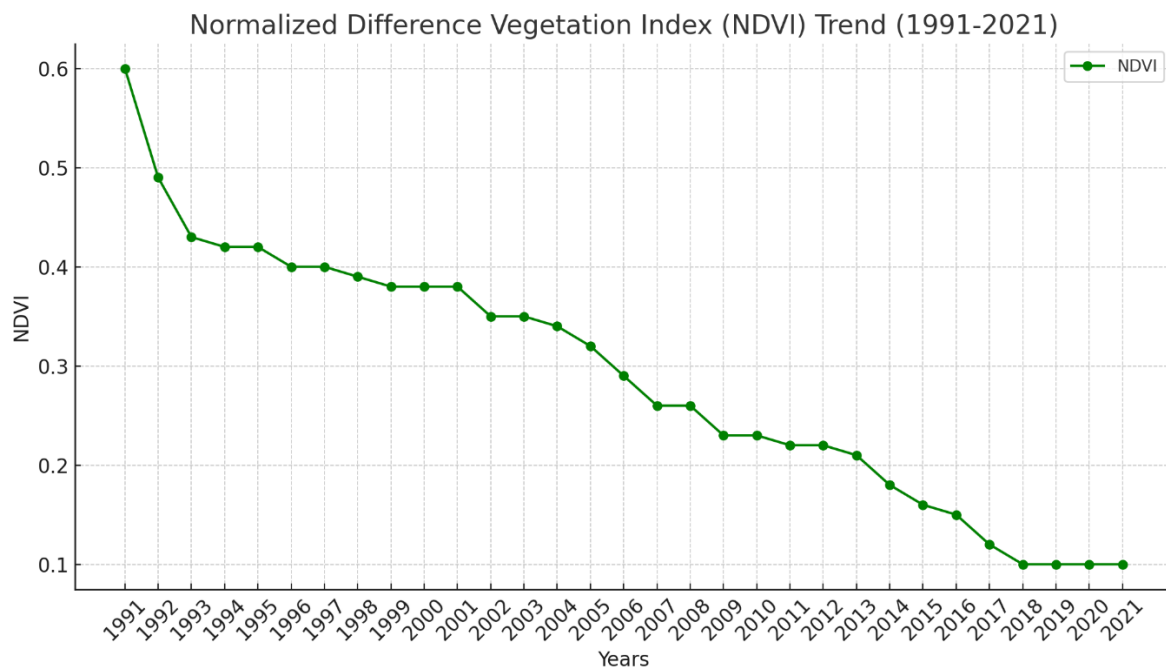


Figure 7: Normalized Difference Vegetation Index Pattern from 1991 – 2021

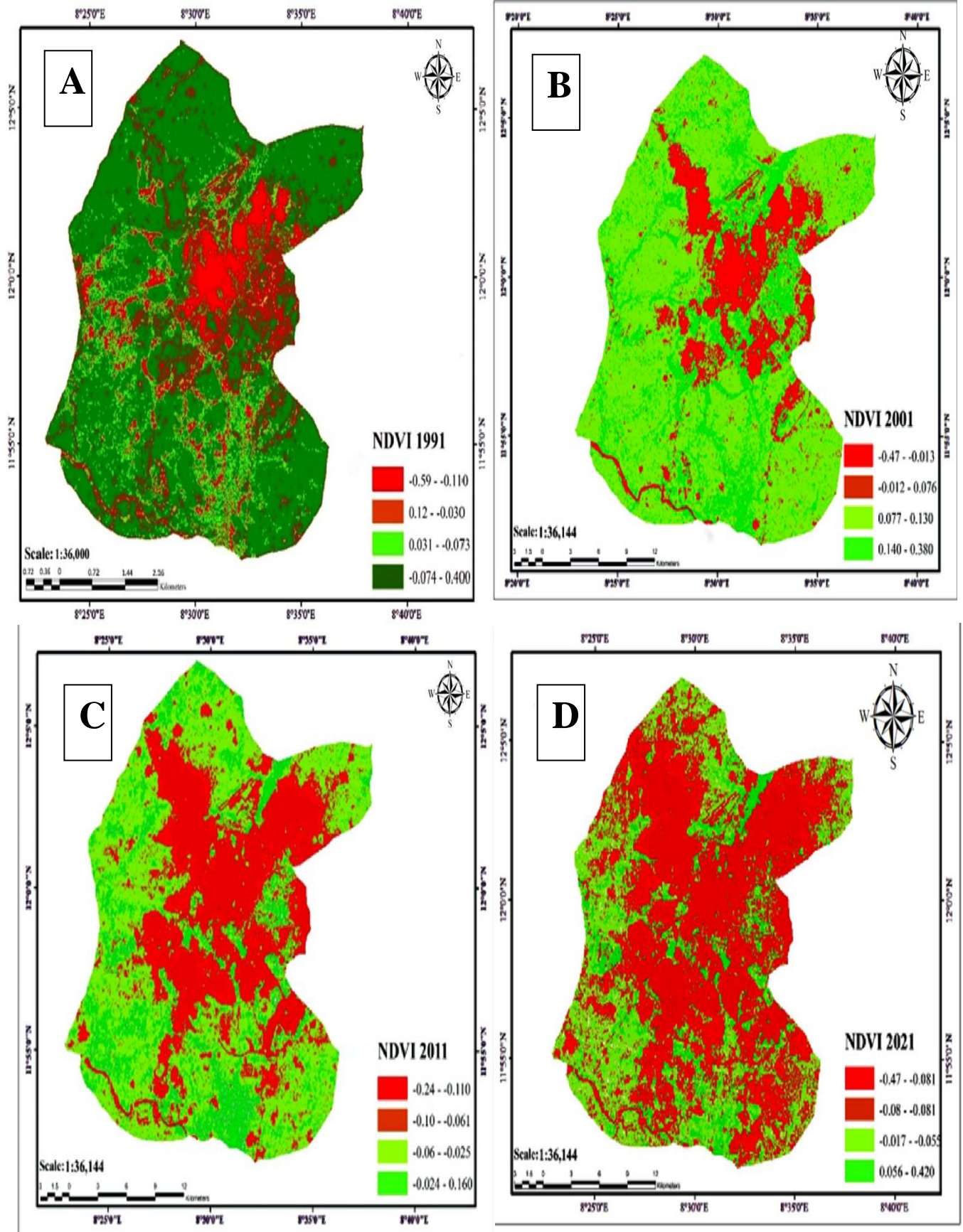


Figure 8: NDVI Map Series from 1991 – 2021 (A=NDVI 1991; B= NDVI 2001; C= NDVI 2011; D= NDVI 2021).

Relationship between pertinent factors affecting land surface temperature

In the evaluation of the relationship between Land Surface Temperature (LST) and factors like bare land, water, built-up areas, and vegetation using Pearson correlation analysis. A positive correlation (r) with built-up areas suggests urbanization increases LST, while a negative correlation with vegetation or water implies they reduce LST. The correlation between LST and built-up areas is statistically significant, with a high correlation coefficient ($r = 0.976838$) and a regression analysis showing that for every square kilometre increase in built-up areas, LST rises by 0.1215°C while increased bare land corresponds to higher LST. These results underscore urbanization's impact on temperature, emphasizing the importance of urban planning and heat mitigation strategies. The study reveals statistically significant relationships between Land Surface Temperature (LST) and various land cover types, emphasizing their impact on urban heat dynamics. Built-up areas show a strong positive correlation with LST ($r = 0.976838$), where each square kilometre increase in built-up areas raises LST by 0.1215°C , highlighting the influence of urban expansion on temperature rise. Bare land also exhibits a robust positive correlation with LST ($r = 0.956586$), signifying its substantial role in elevating temperatures. Conversely, vegetation cover demonstrates a strong negative correlation with LST ($r = -0.940371$), underscoring the cooling effect of

vegetation and its importance in mitigating urban heat islands. Similarly, water bodies ($r = -0.802119$) and the Normalized Difference Vegetation Index (NDVI) ($r = -0.975165$) show strong negative correlations with LST, reflecting their capacity to lower surface temperatures with baseline LST levels indicating the critical need for green spaces and water bodies to moderate urban heat extremes. These findings underscore the importance of sustainable urban planning, incorporating vegetation and water-based strategies, to address the challenges of urban heat islands and climate change adaptation.

This relationship underscores the need for sustainable land management to mitigate urban heat islands and climate change. Consistent with prior research, studies in Nigerian cities such as Sokoto, Lagos, and Kaduna demonstrate urbanization's role in increasing LST (Zaharaddeen *et al.*, 2016; Babalola & Akinsanola, 2016). In Kano, heat islands have emerged in densely developed areas (Tanko *et al.*, 2017; Umar & Satish, 2014), while Abuja and Jos exhibit rising LST due to rapid land use changes (Awuh *et al.*, 2019; Usman *et al.*, 2023). Globally, studies from South Africa, Malaysia, and China further confirm the correlation between LULC and LST, emphasizing the complex dynamics of urbanization and environmental change (Magidi & Ahmed, 2020; Shidiq *et al.*, 2020; Abbas *et al.*, 2021). These findings call for sustainable urban planning to address rising temperatures and climate challenges.

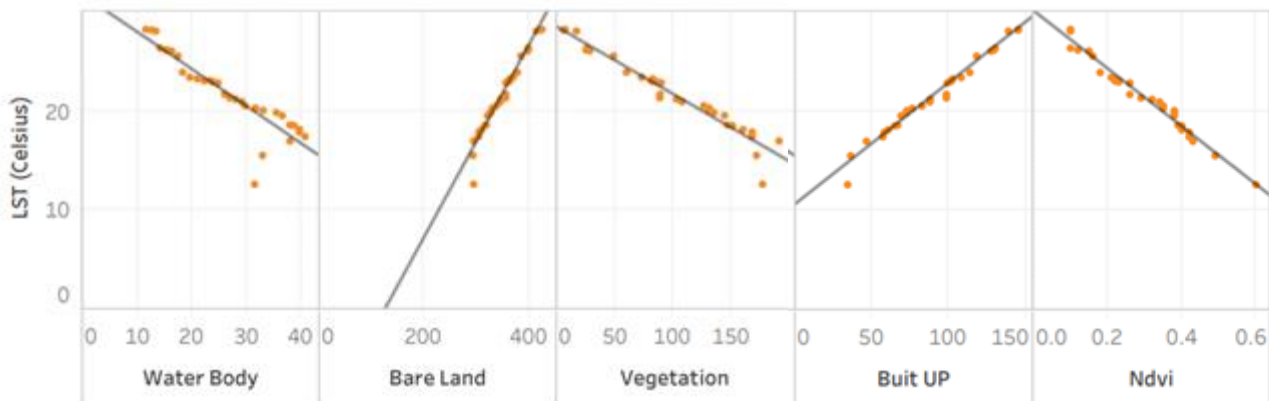


Figure 9: Correlation between LST, NDVI and LULC.

Conclusion

The study provides an extensive yearly analysis of Land Use Land Cover (LULC), Land Surface Temperature (LST), and Normalized Difference Vegetation Index (NDVI) trends in the Kano metropolis from 1991 to 2021. LULC exhibited a steady increase, rising from 33.8 sq km in 1991 to 145.13 sq km in 2021, largely driven by urbanization and socio-economic development. Simultaneously, LST demonstrated a rising trend, peaking at 28°C in 2021 from a low of 12.6°C in 1991, while NDVI declined from 0.6 in 1991 to 0.1 in 2020, reflecting

substantial vegetation loss. Strong correlations were identified, including a positive relationship (0.89) between LULC and LST and a negative correlation between LULC and NDVI with urban expansion contributing significantly to LST, where each square kilometre increase in built-up land adds 0.1215°C to local temperatures. The study emphasizes bare land as another key contributor to LST rise, underscoring the interconnectedness of urban growth, temperature shifts, and vegetation loss. Recommendations focus on sustainable urban planning, afforestation, public awareness, and leveraging GIS for improved

monitoring and policymaking. Additionally, the study demonstrates the effectiveness of Remote Sensing and GIS in environmental analysis, providing valuable insights for climate adaptation and mitigation strategies.

References

- Abbas, A., He, Q., Jin, L., Li, J., Salam, A., Lu, B. & Yasheng, Y. (2021). Spatio-temporal changes of land surface temperature and the influencing factors in the Tarim Basin, Northwest China. *Remote Sensing*, 13(3792). <https://doi.org/10.3390/rs13193792>
- Abdullahi, A., Kibon, U., Rilwanu, T. & Mallam, I. (2016). An analysis of the environmental and health implications of wastewater discharge in Kano metropolis, Nigeria. *Journal Name*, 13, 81–90.
- Aliyu Kasim, A., Mohammed, S., Iyanda, T. & Tanko, I. (2017). Urbanisation effect on the occurrence of urban heat island over Kano metropolis, Nigeria. *International Journal of Scientific and Engineering Research*, 8(9), 293–299.
- Arya Giofandi, E., Munibah, K., Kraugusteliana, K., Novalinda, A. & Sekarrini, C. (2023). The comparison of vector and raster data for the calculation of landscape environment using a geographic information system approach. *IT Journal Research and Development*, 7, 209–219. <https://doi.org/10.25299/itjrd.2022.10878>
- Awuh, M. E., Japhets, P. O., Officha, M. C., Okolie, A. O. & Enete, I. C. (2019). A correlation analysis of the relationship between land use and land cover/land surface temperature in Abuja Municipal, FCT, Nigeria. *Journal of Geographic Information System*, 11, 44–55.
- Babalola, O. S. & Akinsanola, A. A. (2016). Change detection in land surface temperature and land use land cover over Lagos metropolis, Nigeria. *Journal of Remote Sensing & GIS*, 5(3), 1000171.
- Chang, Y., Hou, K., Li, X., Zhang, Y. & Chen, P. (2018). Review of land use and land cover change research progress. *IOP Conference Series: Earth and Environmental Science*, 113, 012087. <https://doi.org/10.1088/1755-1315/113/1/012087>
- Daba, M. H. & You, S. (2022). Quantitatively assessing the future land-use/land-cover changes and their driving factors in the upper stream of the Awash River based on the CA–Markov model and their implications for water resources management. *Sustainability*, 14(3), 1538. <https://doi.org/10.3390/su14031538>
- Edan, M., Maarouf, R. & Hassan, J. (2021). Predicting the impacts of land use/land cover change on land surface temperature using remote sensing approach in Al Kut, Iraq. *Physics and Chemistry of the Earth*, 123, 103012. <https://doi.org/10.1016/j.pce.2021.103012>
- Foody, G. (2020). Explaining the unsuitability of the kappa coefficient in the assessment and comparison of the accuracy of thematic maps obtained by image classification. *Remote Sensing of Environment*, 239, 111630. <https://doi.org/10.1016/j.rse.2019.111630>
- Ibrahim, A., Adewuyi, T. O., Bako, M., Shu'aibu, B., Ajani, A. O. & Akintuyi, O. B. (2024). GIS-based multi-criteria land suitability mapping for sorghum production in south-eastern parts of Niger State, Nigeria. *Environmental Technology and Science Journal*, 15(1). <https://dx.doi.org/10.4314/etsj.v15i1.3>
- Ibrahim, A. M. & Mohammed, M. A. (2016). Road network: The silent treasures of Kano metropolis. *Bayero Journal of Pure and Applied Sciences*, 9(1), 87–92. <https://doi.org/10.4314/bajopas.v9i1.14>
- Jabbar, H., Hamoodi, M. & Al-Hameedawi, A. (2023). Urban heat islands: A review of contributing factors, effects, and data. *IOP Conference Series: Earth and Environmental Science*, 1129, 012038. <https://doi.org/10.1088/1755-1315/1129/1/012038>
- Koko, A. F., Wu, Y., Abubakar, G. A., Alabsi, A. A. N., Hamed, R. & Bello, M. (2021). Thirty years of land use/land cover changes and their impact on urban climate: A study of Kano metropolis, Nigeria. *Land*, 10(11), 1106. <https://doi.org/10.3390/land10111106>
- Lai, S., Leone, F. & Zoppi, C. (2020). Spatial distribution of surface temperature and land cover: A study concerning Sardinia, Italy. *Sustainability*, 12(8), 3186. <https://doi.org/10.3390/su12083186>
- Magidi, J. & Ahmed, F. (2020). Spatio-temporal variations of land surface temperature using Landsat and MODIS: Case study of the City of Tshwane, South Africa. *South African Journal of Geomatics*, 9(2), 379. Based on the information available, the complete reference in APA format is:
- Mohiuddin, G. & Mund, J.-P. (2024). Spatiotemporal analysis of land surface temperature in response to land use and land cover changes: A remote sensing approach. *Remote Sensing*, 16(7), 1286. <https://doi.org/10.3390/rs16071286>
- Musa, U. & Kumar, S. (2015). Spatial and temporal changes of urban heat island in Kano metropolis, Nigeria. *Journal of Engineering Science and Technology*, 1, 20.
- Nuruzzaman, M. (2015). Urban heat island: Causes, effects, and mitigation measures—A review. *International Journal of Environmental Monitoring and Analysis*, 3(2), 67–73. <https://doi.org/10.11648/j.ijema.20150302.15>
- Patel, S., Indraganti, M. & Jawarneh, R. (2023). A comprehensive systematic review: Impact of land use/land cover (LULC) on land surface temperatures (LST) and outdoor thermal comfort.

- Building and Environment*, 249, 111130. <https://doi.org/10.1016/j.buildenv.2023.111130>
- Roy, P. & Roy, A. (2010). Land use and land cover change: A remote sensing & GIS perspective. *Journal of the Indian Institute of Science*, 90, 489–502.
- Sajib, M. Q. U. & Wang, T. (2020). Estimation of land surface temperature in an agricultural region of Bangladesh from Landsat 8: Intercomparison of four algorithms. *Sensors*, 20(6), 1778. <https://doi.org/10.3390/s20061778>
- Tanko, I. A., Suleiman, Y. M., Yahaya, T. I. & Kasim, A. A. (2017). Urbanisation effect on the occurrence of urban heat island over Kano metropolis, Nigeria. *International Journal of Scientific & Engineering Research*, 8(9), 293.
- Yang, J., Ren, J., Sun, D., Xiao, X., Xia, C., Jin, C. & Li, X. (2021). Understanding land surface temperature impact factors based on local climate zones. *Sustainable Cities and Society*. <https://doi.org/10.1016/j.scs.2021.102818>
- Zaharaddeen, I., Ibrahim, I., Baba, A. & Zachariah, A. (2016). Estimation of land surface temperature of Kaduna metropolis, Nigeria using Landsat images. *Science World Journal*, 11(3).
- Zitta, S. W. & Akinseye, S. A. (2020). Assessment of urban heat island using remote sensing and GIS techniques in Jos metropolis, Nigeria. *FUDMA International Journal of Social Sciences (FUDIJOSS)*, 2(2), 29–40.